British Journal of Applied Science & Technology
18(4): 1-18, 2016; Article no.BJAST.28836
ISSN: 2231-0843, NLM ID: 101664541

SCIENCEDOMAIN *international*
www.sciencedomain.org

Protection of J55 Steel Surface in Acidic Well Treatment Fluids Using Green Anticorrosive Oilfield Chemicals from 5-hydroxytryptophan

Ekemini Ituen[1,2*], Onyewuchi Akaranta[2,3] and Abosede James[3]

[1]Materials Physics and Chemistry Research Laboratory, College of Science, China University of Petroleum, Qingdao 266000, China.
[2]African Centre of Excellence for Oilfield Chemicals Research (ACE-CEFOR), Institute of Petroleum Studies, University of Port Harcourt, Nigeria.
[3]Department of Pure and Industrial Chemistry, University of Port Harcourt, Nigeria.

Authors' contributions

This work was carried out in collaboration between all authors. All the authors contributed in the design of the study. Author EI performed the experiments, analyzed and interpreted the results, wrote the first draft of the manuscript and managed literature searches under guidance and supervision of authors OA and AJ. All authors read and approved the final manuscript.

Article Information

DOI: 10.9734/BJAST/2016/28836
Editor(s):
(1) Aleksey Aleksandrovich Hlopitskiy, Department of Technology Inorganic Substances, Ukrainian State University of Chemical Technology, Ukraine.
Reviewers:
(1) Kashif Rahmani Ansari, Indian Institute of Technology (BHU) Varanasi, India.
(2) Vanessa de Freitas Cunha Lins, Federal University of Minas Gerais, Brazil.
(3) Roseana Florentino da Costa Pereira, Federal Institute of Pernambuco, Brazil.
Complete Peer review History: http://www.sciencedomain.org/review-history/17573

Original Research Article

Received 9th August 2016
Accepted 25th September 2016
Published 21st January 2017

ABSTRACT

A non-toxic compound, 5-hydroxytryptophan (5-HTP), was investigated for its performance as inhibitor of J55 steel corrosion in both 1M and 15% HCl for the first time. The efficiency was determined using Weight Loss (WL), Electrochemical Impedance Spectroscopy (EIS) and Potentiodynamic Polarization (PDP) techniques. Inhibition efficiency obtained from WL measurement decreased from 91.4% and 73.9% in 1 M and 15% HCl respectively at 30℃ to 67.4% and 40.3% in the respective acid solutions at 90℃. B lending 5-HTP with potassium iodide, polyethyleneglycol and glutathione increased the efficiency to values above 72% in both acid solutions at 90℃. The inhibitor adsorption was spont aneous and physical in mechanism, following

**Corresponding author: E-mail: ebituen@gmail.com;*

the Langmuir adsorption model. Adsorption was also exothermic with resultant decrease in entropy of the bulk solution. Increase in 5-HTP concentration increased the charge transfer resistance but decreased the double layer capacitance. Tafel polarization study shows that 5-HTP behaves as mixed type inhibitor with anodic predominance. The corrosion products and metal surface were analysed using other techniques like SEM/EDS, FTIR, UV-VIS. The surface protection is attributed to formation of protective film of 5-HTP molecules on J55 steel surface facilitated by O, N and C=C functionalities. The resulting oilfield chemicals can be used as efficient alternative corrosion inhibitors for protection of surface and downhole steel construction materials.

Keywords: 5-hydroxytryptophan; oilfield chemicals; acid corrosion inhibitor; EIS; SEM/EDS; J55 steel.

1. INTRODUCTION

A number of chemicals are required in oil and gas production. These chemicals are referred to as oilfield chemicals. From the drilling and cementing to recovery, transportation and refining, several oilfield chemicals are employed. In most cases, when existing wells deplete, the use of chemistry to maintain production through well stimulation, secondary and enhanced oil recovery operations, becomes very crucial. Oilfield chemicals include those additives for the drilling mud, fluid loss additives, clay stabilizers, lubricants, biocides, corrosion inhibitors, scale inhibitors, gelling agents, filter cake removal agents, hydrate control agents, cement additives, etc. Many fluids such as fracturing, flooding, stimulation, and pickling contain acid which stimulates corrosion of associated metallic structural materials. Corrosion gulps a major part of production cost in the oil and gas industry. The National Association of Corrosion Engineers (NACE) estimated the direct cost of corrosion in U.S.A. at $276 billion in 1998 which was approximately 3.1% of the gross domestic product (GDP) [1] but exceeded $1trillion in 2012 [2]. Globally, the annual cost of corrosion worldwide is estimated at $ 2.2 trillion (2010), which is roughly 3% of world's GDP [3]. Obot [4] opines that the expenditure on corrosion could have been channeled to provide food for the poor as part of the Millennium Development Goals (MDGs). Therefore, the need to device cheaper means to control corrosion and cut down the associated cost cannot be overemphasized.

An easy and cost effective way of combating oilfield corrosion is the use of corrosion inhibitors. Thus, corrosion inhibitors are an important class of oilfield chemicals. They can be used as additives in drilling, acidizing, fracture, stimulation, and enhanced oil recovery fluids to reduce the rate of corrosion. These fluids usually contain corrodible agents like acid (HCl), water and carbon(iv)oxide [5-6]. Selection of the corrosion inhibitor requires consideration of some important factors like sustainability of its source(s), cost of raw materials, its chemistry and environmental impacts [7]. Many compounds that contain functionalities like nitrogen, oxygen, multiple bonds, conjugated double bond systems, heteroatoms and aromatic rings have been found to be efficient CIs for different metals in various media [8-13]. However, some of these compounds may be toxic or very expensive. There are also some efficient non-toxic CIs that have been reported in literature [14-15] but some of them are very expensive to buy or synthesize. Thus, CIs sourced from cheap, sustainable and non-toxic materials would be desirable. Nigeria is blessed with numerous local resources from where CIs could be sourced. Sourcing CIs from local materials would in addition create internal wealth, reduce importation, and help to actualize the Nigerian Content Act. This Act entails value added or created in Nigerian economy through utilization of Nigerian resources for provision of goods and services to petroleum industries, within acceptable quality, health, safety and environmental standards in order to stimulate development of indigenous capability [16]. Since there is still little or no progress made in that direction so far, this study aims to achieve this contribution.

5-HTP has been reported as the active compound in seeds of *Griffonia simplicifolia*. Ultra Performance Liquid Chromatography and High Performance Liquid Chromatography direct assays of *Griffonia simplicifolia* have been reported to yield about 20% (seeds); 0.3-1.2% (leaves) and 0.1-0.2% (pods) of naturally occurring 5-HTP [17]. *Griffonia simplicifolia* is a shrub, leguminous plant which grows abundantly in many southern parts of Nigeria. It can be propagated by seed and by wildings. It has been classified taxonomically [18] with a scientific name: *Griffonia simplicifonia* (DC.) Bail, which is synonymous to *Bandeiraea simplicifolia* (DC.) Bail, and local names such as Children whistle, *Arin, Olabahun, Tapara, Alukoko and Mba-aba.* The seeds or leaves of the plant have been used

for treatment of various health challenges especially in folk medicine. Some of these treatment include diarrhea, vomiting and stomach ache, wounds, bladder and kidney ailments [18], anxiety and depression, insomnia, migraine and headache [18,19], sickle cell [20], Ehrlich Ascites tumor cells [21], etc. Most of these uses have been attributed to the presence of 5-hydrotryptophan (5-HTP), the major/active alkaloid in the plant [18,19]. The 5-HTP is not toxic and can be obtained in large quantity from local source [19] or prepared cheaply from tryptophan [22,23]. Besides, 5-HTP contains similar electronic functionalities mentioned above in its molecular structure (see Fig. 1).

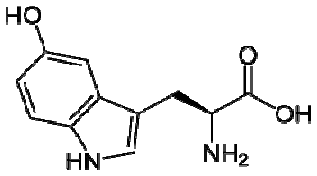

Fig. 1. Chemical structure of 5-HTP

In this study, 5-HTP was investigated as alternative CI for J55 steel in both 1 M HCl and 15% HCl for the first time. The 15% HCl is used to simulate real field acidizing concentration while 1 M HCl is a concentration many researchers have used to test their CIs [24-27]. The choice of HCl is motivated by its widespread use in well acidizing and enhanced oil recovery fluids. The J55 steel coupons are used to simulate oil transfer steel tubings, oil drilling pipes, casings, line pipes, etc., encountered in the oilfield [28,29]. Standard techniques like gravimetric and electrochemical measurements are used to evaluate the CI efficiency [30,31]. The morphology (pittings or roughness) of the metal specimen is checked by SEM to observe possible difference with and without the inhibitor. Other techniques like FTIR, UV-VIS, EDS are employed to further characterize the inhibition phenomenon. The 5-HTP was also blended with some compounds for improved performance at high temperature. Adsorption, kinetic and thermodynamic models are also used to further explain the inhibitor interaction with metal surface.

2. MATERIALS AND METHODS

2.1 Materials

Weights were measured using Sartorius CPA225D analytical balance with sensitivity ±0.00001g. Gamry ZRA REF 600-18042 Potentiostat/ Galvanostat was used for electrochemical measurements. The 756PG UV-Vis Spectrophotometer, supplied by Shanghai Spectrum Instruments Co., Ltd and TENSOR II FTIR Spectrophotometer were also used for spectroscopic assessments. The SEM/EDS was AMETEX S4800 EDAX TSL. Different grades of silicon carbide papers such as CC-22F P2000, P1000, P500, P400, P200 and P100 were used for surface abrasion.

2.2 Preparation of Steel Specimens

The J55 steel specimens were supplied by Qingdao Tengxiang Instrument and Equipment Co. Ltd, China. They were mechanically press-cut into coupons of dimension 2 cm x 2 cm for gravimetric experiments; 1 cm x 1 cm for electrochemical studies and 2 cm x 1 cm for surface analysis. The surface was treated as provided by NACE Recommended Practice RP-0775 and ASTM G-1 & G-4 for surface finishing and cleaning. In addition coupons for electrochemical studies were abraded with various grades of silicon carbide paper and finished to mirror surface with CC-22F P2000 grade. The prepared specimens were enclosed in sealed water-proof bags and stored in moisture free desiccator prior to use. The chemical compositions (wt. %) of J55 steel was C (0.24), Si (0.22), Mn (1.1), P (0.103), S (0.004), Cu (0.5), Ni (0.28), Mo (0.019), Fe (balance).

2.3 Preparation of Inhibitor Solutions

Analytical grade HCl was diluted to concentrations of 1 M and 15% using double-distilled water. Powdered 5-hydroxytryptophan (HPLC 99.9%, extracted from seeds of *Griffonia simplicifolia*) was supplied by Shaanxi Kanglai Ecology Agriculture Co. Ltd., China and was used as supplied without further analyses. The 5-HTP was prepared to five different concentrations ($1x10^{-5}$, $3x10^{-5}$, $5x10^{-5}$, $8x10^{-5}$ and $10x10^{-5}$ M) in the HCl solutions. The test solutions were used for the study about 48 hours after preparation.

2.4 Preparation of Inhibitor Blends

The additives used in this study were: polyethyleneglycol (PEG-4000, Industrial grade) supplied by Richest group Ltd., Shangai; sodium gluconate (Analytical grade) and glutathione (Industrial grade) supplied by Wuhan Yuancheng Gongchuang Technology Co. Ltd., China; and potassium chloride (Analytical grade) supplied by Meyer Chemical Technology Co. Lt., Shangai;

China. They were used as supplied without further analyses. The concentration of each additive used was $1x10^{-6}$ M. They were blended with $10x10^{-5}$ M 5-HTP and prepared in the HCl with vigorous stirring. The resulting blend solution was allowed to stand for 48 hours with regular agitation at about 6 hours interval before use in the corrosion study.

2.5 Weight Loss Technique

Pre-weighed steel coupons were immersed in the acid solutions without and with different concentrations of 5-HTP for five hours interval maintained at 30℃ in a water bath. They were retrieved, washed in 20% NaOH solution containing about 200 g/L of zinc dust until clean, dried in air after rinsing in acetone and weighed to determine the weight loss. Experiments were carried out in triplicates but only the mean values of the weight losses (g) are reported. The initial and final weights of the coupons were denoted as w_1 and w_2 respectively, corrosion rate of iron (R), percentage inhibitor effectiveness (inhibition efficiency), $\mathcal{E}_{WL}$, and degree of surface coverage (θ), were calculated as follows:

$$R = \frac{87.6(w_1 - w_2)}{\rho A t} \quad (1)$$

$$\mathcal{E}_{WL} = 100\left(\frac{R_b - R_i}{R_b}\right) \quad (2)$$

$$\theta = 0.01\mathcal{E}_{WL} \quad (3)$$

where R_b and R_i are the corrosion rates (cmh^{-1}) in the absence and presence of the inhibitor, ρ is the density of iron, A is the average surface area (cm^2) of the metal specimens and t is the immersion time (h). The values of corrosion rate obtained were converted to another unit (mmpy) using conversion factors explained in literature [32]. This procedure was repeated at other temperatures like 45℃, 60℃, 75℃ and 90℃ in the different test solutions.

2.6 Electrochemical Measurements

The conventional three electrode set up was used consisting of saturated calomel electrode (SCE) as reference electrode, platinium as counter electrode and J55 steel coupons as working electrode. The EIS were conducted at frequency of 10^5 to 10^{-2} Hz for open circuit immersion time of 30 minutes at 30℃. The voltage was changed to -0.15V to +0.15V vs. E_{OC} at scan rate of 1 mV/s for PDP measurements [33,34]. EChem software package was used for data fitting and analyses.

Charge transfer resistance from EIS measurements were used to compute the inhibition efficiency according to Eq. 4. The inhibition efficiency (from PDP data) was calculated from the corrosion current densities using Eq. 5.

$$\mathcal{E}_{EIS} = 100\left(\frac{R_{ctI} - R_{ctB}}{R_{ctI}}\right) \quad (4)$$

where R_{ctB} and R_{ctI} are charge transfer resistances in the absence and presence of inhibitor respectively.

$$\mathcal{E}_{PD} = 100\left(1 - \frac{I^i_{corr}}{I^b_{corr}}\right) \quad (5)$$

where I^b_{corr} and I^i_{corr} are the corrosion current densities in the absence and presence of the inhibitor respectively. The magnitude of the double layer capacitance (C_{dl}) of the adsorbed film was calculated from constant phase element (CPE) constant (Y_o) and charge transfer resistance (R_{ct}) using Eq. 6.

$$C_{dl} = (Y_0 {R_{ct}}^{n-1})^{\frac{1}{n}} \quad (6)$$

where n is a constant showing degree of roughness of the metal surface obtained from the phase angle given that $(j^2 = -1)\alpha$ is the phase angle of CPE and $n = 2\alpha/\pi$) is the CPE exponent.

2.7 UV-vis Study

The UV-vis spectrum was first obtained using the solution containing $10x10^{-5}$ M 5-HTP in 1 M HCl prior to immersion of the J55 steel. Another spectrum was obtained using a solution resulting from immersing the steel in 1 M HCl for 24 hours. The spectral profiles were then compared.

2.8 FTIR Study

The FTIR spectrum of the pure 5-HTP sample was obtained. Another spectrum of the 5-HTP film formed on J55 steel surface after immersion (both mixed with potassium bromide) was recorded. Both spectra were compared.

2.9 SEM/EDS Study

Steel coupons of sizes 1 cm x 2 cm were abraded to mirror finish as earlier described. The SEM images were recorded in the vacuum mode before and after immersion in HCl. This was repeated with a coupon immersed in HCl

containing $10x10^{-5}$ M 5-HTP solution. The instrument was operated at 5 kV. Also, EDS profiles of the steel surface *ab initio* and the corrosion products of three points each metal surface sample in the inhibited and uninhibited solutions were recorded.

3. RESULTS AND DISCUSSION

3.1 Weight Loss Measurement

The corrosion rate of J55 steel in both the 1 M and 15% HCl were calculated from weight loss data and used to compute the inhibition efficiency (%I) and fractional surface coverage (θ). Results obtained with and without different concentrations of 5-HTP are presented in Table 1.

3.1.1 Effect of corrosive fluid concentration

The efficiency of 5-HTP was tested both 1 M HCl and 15% HCl (4.4 M HCl) and the results obtained (Table 1) were compared. Results show that the effectiveness of 5-HTP declined when the acid concentration was increased from 1 M to 15%. For instance, the inhibition efficiency decreased from 91.42% in 1 M HCl to 73.94% in 15% HCl at 30℃. This represents about 18.03% decrease in inhibition efficiency on about 340% increase in acid concentration. Though the inhibition efficiency reduces due to increased acid strength, the value is still reasonably high for a bio-based material and can be optimized to obtain higher efficiency using intensifiers. This result demonstrates that 5-HTP can protect J55 steel materials in less aggressive media to highly aggressive media.

3.1.2 Effect of concentration of inhibitor

The obtained inhibition efficiency increased as concentration of 5-HTP was increased at constant temperature (Table 1). Similar trends have been reported in literature [35,36]. This implies that as number of molecules of 5-HTP in the acid solution increases, more 5-HTP molecules are adsorbed on the steel surface and its degree of protection is improved. Consequently, it may be possible to achieve higher inhibition efficiencies by further increasing the concentration of 5-HTP. However, CIs are usually deployed in small quantities hence using too much or too small quantity of the inhibitor is not desirable [7]. A concentration of $10x10^{-5}$ M corresponds to just 22 mg of 5-HTP per 1L of acid solution, which is reasonably small [32].

3.2 Inhibitor Sensitivity to Downhole Temperature Difference

Recently, some industries have ventured into production/recovery of hydrocarbons from deep pay zones. Difference between surface and downhole temperatures is a key factor that influences the effectiveness of corrosion inhibitors used for such operations. Going down the well, the difference in temperature per unit well length has been described as geothermal gradient. An average geothermal gradient of about 25℃ per km of depth (1℉ per 70 feet of depth) is believed to be universal [37]. From literature reports, the average geothermal gradient in Niger delta fields is 28℃/km [38]. Many deep wells in the region are estimated to be about 2-4 km deep corresponding to downhole temperature in the range of 65℃-125℃ [39,40].

To elucidate the effect of temperature on the performance of 5-HTP, the highest concentration of the inhibitor was tested at five different temperatures between 30℃ and 90℃. Results obtained are shown in Table 2. It can be observed from the table that inhibition efficiency decreased as temperature increased. For instance, in 1 M HCl solution, the inhibition efficiency reduced from 91% at 30℃ to 67% at

Table 1. Corrosion rate, inhibition efficiency and fractional surface coverage data for the inhibition of J55 steel corrosion in 1M and 15% HCl using different concentrations of 5-HTP at 30℃

Test solution	In 1M HCl			In 15% HCl		
	R (mmpy)	ε_{WL}(%)	θ	R (mmpy)	ε_{WL}(%)	θ
Blank solution	33.82	-	-	161.02	-	-
1 x 10^{-5} M	6.07	82.04	0.82	68.32	60.14	0.60
3 x 10^{-5} M	5.71	83.11	0.83	59.46	63.07	0.63
5 x 10^{-5} M	4.70	86.09	0.86	58.04	66.14	0.66
8 x 10^{-5} M	3.89	88.47	0.88	49.01	69.56	0.70
10 x 10^{-5} M	2.90	91.42	0.91	44.67	73.94	0.74

90℃. The *%I* obtained were even lower in 15% HCl compared to 1 M HCl at high temperatures. This implies that if 5-HTP is used as CI in acidizing fluid, it will perform effectively at surface conditions and loose efficiency some kilometers downhole. In literature, this trend is associated with physical adsorption mechanism [41]. To improve the performance of 5-HTP at high temperature, it can be blended with synergistic additives [7].

3.3 Performance of 5-HTP and Intensifier Blends

There are various reports that certain substances (called intensifiers) can increase the inhibition efficiency of some corrosion inhibitors. Many of such intensifiers have been listed [7,42]. Intensifiers are required because CIs frequently do not provide adequate protection to steels at high temperatures and long exposure time [43]. The efficiency of 5-HTP obtained in this study was low at high temperature, hence it was blended potassium iodide (KI), polyethylene glycol (PEG), sodium gluconate (NaG), and glutathione (GLU).

The results obtained (Tables 3-4) show that the inhibition efficiency improved at high temperatures. For instance, at 90℃, the blends containing PEG, KI and GLU afforded %I of 88%, 87% and 92% respectively in 1M HCl and 72%, 73%, and 76% in 15% HCl. This demonstrates that the inhibitor blends could be efficient in various oilfield acidizing procedures associated with high temperature operations.

Table 2. Effect of temperature on the inhibition efficiency of 5-HTP as corrosion inhibitor for J55 steel in acidic solutions

T(℃)	%I in 1 M HCl	%I in 15% HCl
30	91.42	73.94
45	88.02	69.43
60	81.14	63.17
75	76.16	54.01
90	67.42	40.30

3.4 Adsorption Study

Corrosion Inhibitors are generally believed to act by adsorption on the metal surface. The adsorption can occur through electrostatic interactions between charged species of the inhibitor and metal surface (physisorption) or by actual chemical interaction between the CI functional group(s) and metal orbitals (chemisorption) [41]. To elucidate this mechanism, the fractional surface coverage (θ) data were usually fitted into adsorption isotherm models as done in literature [44]. Some parameters were deduced from the plots and used to explain the nature of interaction between the CI and metal surface. The isotherm models tested were those proposed by Langmuir, Temkin, Freundlich, Flory Huggins and El-Awady et al. The best fit was obtained with

Table 3. Effect of Intensifiers on inhibition efficiency (%) of 5-HTP on J55 steel in 1M HCl solution

T(°C)	5-HTP Only	5-HTP + KI	5-HTP +PEG	5-HTP +NaG	5-HTP + GLU
30	91.4	99.0	98.8	93.5	99.3
45	88.0	98.0	97.7	90.1	99.0
60	81.1	96.3	95.5	84.7	98.1
75	76.8	92.0	91.1	78.4	96.4
90	67.4	88.1	87.0	69.1	92.0

Table 4. Effect of Intensifiers on inhibition efficiency (%) of 5-HTP on J55 steel in 15% HCl solution

T(°C)	5-HTP Only	5-HTP + KI	5-HTP +PEG	5-HTP +NaG	5-HTP + GLU
30	73.9	87.8	86.1	76.0	90.2
45	69.4	85.4	84.0	74.0	86.7
60	63.2	81.1	80.0	70.7	82.2
75	54.0	77.2	77.4	66.5	79.4
90	40.3	72.1	73.4	62.1	75.9

Langmuir isotherm (Figs. 2-3) with $R^2 \geq$ 0.99725. The expression for the model is given in Eq. 7.

$$\frac{C_{inh}}{\theta} = \frac{1}{K_{ads}} + C_{inh} \quad (7)$$

where C_{inh} is the concentration of inhibitor (moldm^{-3})in the acid solution and K_{ads} is the adsorption-desorption equilibrium constant which can be used to determine the free energy change of adsorption (ΔG_{ads}) according to Eq. 8.

$$\Delta G_{ads} = -RT \ln(55.5K_{ads}) \quad (8)$$

where 55.5 represents the concentration of water molecules displaced by inhibitor molecules at the surface [45], R is the universal gas constant and T is the absolute temperature. The slopes of the graphs are not exactly unity as provided by the Langmuir isotherm model. This may be attributed to interactions between the 5-HTP molecules or formation of more than one layer of 5-HTP on the J55 steel surface. These are conditions that were ignored during the derivation of the model. The values of K_{ads} and ΔG_{ads} obtained are given in Table 5. The constant, K_{ads} relates to the strength of inhibitor-metal surface interaction. It can be observed that K_{ads} decreases as temperature increases which implies that the adsorptive binding strength of 5-HTP on J55 steel decreases as temperature increases, perhaps due to desorption of its molecules from the surface. The values also decrease in 15% than 1 M HCl demonstrating decreased strength of adsorption with increased solution aggressiveness. The ΔG_{ads} values are between -9.42 kJmol^{-1} to -14.10 kJmol^{-1} which fall within the range for physical adsorption mechanism, indicating that the adsorptive film has an electrostatic character [45,46].

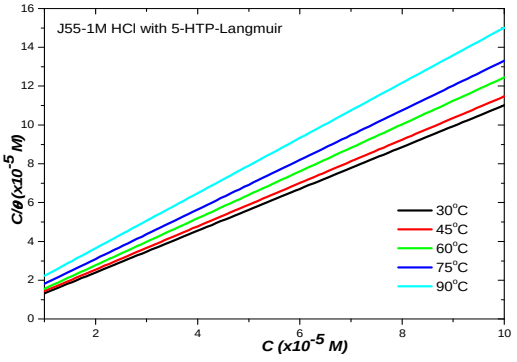

Fig. 2. Langmuir adsorption isotherm for the inhibition of J55 steel corrosion in 1 M HCl by different concentrations of 5-HTP at 30℃ to 90℃

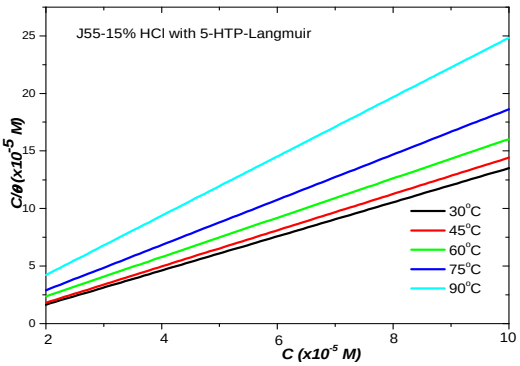

Fig. 3. Langmuir adsorption isotherm for the inhibition of J55 steel corrosion in 15% HCl by different concentrations of 5-HTP at 30℃ to 90℃

3.5 Kinetic and Thermodynamic Considerations

In all the systems tested, corrosion rate increased as temperature increased. The corrosion rate data were fitted into Arrhenius kinetic model (Eq. 9) and activation energy was elucidated from linear plots of $\log CR$ against reciprocal of temperature (Fig. 4). The obtained activation energy increased on addition of the inhibitor depending on inhibitor concentration. Based on the concept of activation and collision theory, it can be considered that before the acid solution corrodes the metal surface, molecules of the acid must collide with the metal molecules on the surface. The acid molecules should possess energy up to a minimum threshold called the activation energy.

$$\log R = \log A - \frac{E_a}{2.303RT} \quad (9)$$

where E_a is the activation energy, A the Arrhenius pre-exponential factor or frequency facto, R Is the universal gas constant and T is absolute temperature. In the presence of the inhibitors, the activation energy was found to increase (Table 6). This implies that the acid molecules must acquire extra (higher) energy in the inhibited solution for corrosion to occur, hence corrosion inhibition. Therefore, addition of 5-HTP deepens the energy barrier well and increases the activation energy. The activaton energy was lower in 15% HCl than 1 M HCl indicating that molecules of 15% HCl solution require less energy barrier to cross the activated complex and form corrosion products with mild steel than those of 1 M HCl. The increase in

activation energy in the presence of inhibitor in both acids is consistent with trends reported in literature and is associated with physical adsorption mechanism [47,48].

The other activation parameters given in Table 6 were derived from the transition state equation (Eq. 10). Linear plots of $\log(\frac{CR}{T})$ against reciprocal of temperature (Fig. 5).

$$\log(\frac{CR}{T}) = \left[\left(\log\left(\frac{R}{Nh}\right) + \left(\frac{\Delta S^*}{2.303R}\right)\right)\right] - \left(\frac{\Delta H^*}{2.303RT}\right) \quad (10)$$

where ΔH^* and ΔS^* are the enthalpy and entropy change of activation respectively. The values of ΔS^* are all negative which implies that a decrease in disorderliness of the system takes place on moving from reactants to activated complex [49]. It also indicates that the activated complex in the rate determining step involves an

Table 5. Parameters deduced from Langmuir adsorption isotherm

T(℃)	1 M HCl			15% HCl		
	$slope$	K_{ads} (M^{-1})	ΔG_{ads} ($kJmol^{-1}$)	$slope$	K_{ads} (M^{-1})	ΔG_{ads} ($kJmol^{-1}$)
30	1.42	4.16	-13.71	1.32	0.76	-9.42
45	1.27	3.23	-13.72	1.28	0.74	-9.82
60	1.21	2.94	-14.10	1.04	0.66	-9.97
75	1.11	1.89	-13.46	1.04	0.66	-10.42
90	1.07	1.25	-12.79	0.96	0.57	-10.42

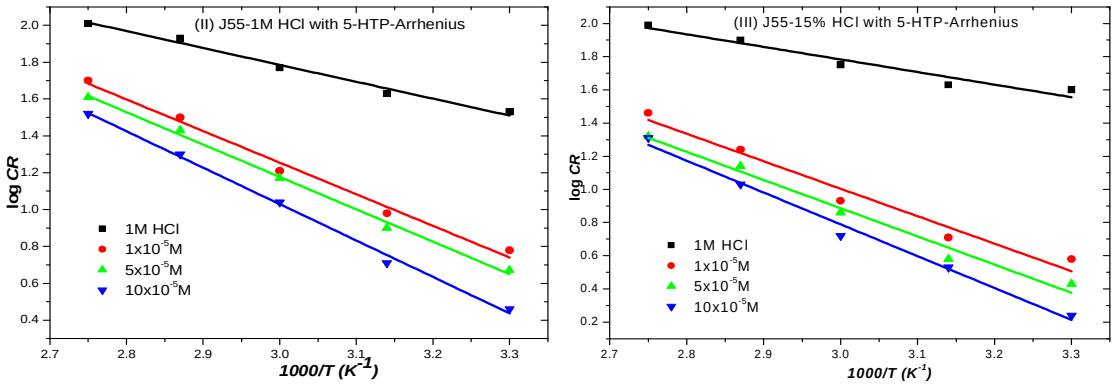

Fig. 4. Arrhenius plot for the inhibition of corrosion of J55 steel in 1 M HCl using different concentrations of 5-HTP

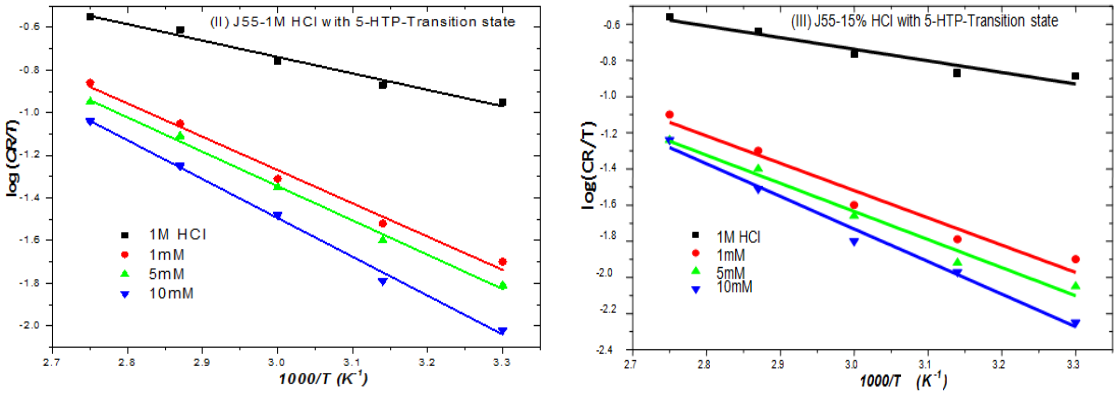

Fig. 5. Transition state plot for the corrosion of J55 steel in 1 M HCl in the absence and presence of different concentrations of 5-HTP

association of inhibitor on metal surface instead of dissolution of the metal. The negative sign of ΔH^* reflects the exothermic nature of J55 steel corrosion in HCl. A spontaneous exothermic phenomenon with a decrease in entropy is thermodynamically consistent at all temperatures studied, showing that the results obtained are consistent.

Table 6. Activation parameters for corrosion of mild steel in both 1 M HCl containing different concentrations of 5-HTP at 30℃ to 90℃

Conc ($x10^{-5}$M)	In 1 M HCl		
	E_a (kJmol^{-1})	ΔH^* (kJmol^{-1})	ΔS^* (kJmol^{-1})
0	17.56	-14.74	-0.18
1	32.83	-29.87	-0.15
5	33.64	-30.83	-0.15
10	37.83	-34.85	-0.14

Table 7. Activation parameters for corrosion of mild steel in both 1 M 15% HCl containing different concentrations of 5-HTP at 30℃ to 90℃

Conc ($x10^{-5}$M)	In 15% HCl		
	E_a (kJmol^{-1})	ΔH^* (kJmol^{-1})	ΔS^* (kJmol^{-1})
0	9.23	-15.06	-0.14
1	12.49	-32.49	-0.11
5	27.44	-48.29	-0.10
10	28.21	-62.16	-0.08

3.6 Electrochemical Impedance Spectroscopy

EIS analyses of 1 M HCl without and with three different concentrations 5-HTP and the Nyquist and Bode plots shown in Fig. 6 were obtained. The semicircles obtained from Nyquist plots are imperfect and the sizes of diameters are influenced in the presence of 5-HTP from that of the free acid solution. The difference in sizes of their diameters demonstrates that 5-HTP has influence on corrosion of J55 steel due to inhibition. The diameters increase as inhibitor concentration increases following the same trend as inhibition efficiency. The imperfection in the shape of the semicircle can be attributed to surface roughness of the J55 steel. The single capacitive loop obtained indicates that the mechanism of corrosion is controlled mainly by charge transfer process [48]. The shapes of the plots were similar in both inhibited and free acid solution demonstrating that the mechanism of steel corrosion is not influenced by introduction of 5-HTP. The equivalent circuit shown in Fig. 7 gave the best fit for the experimental data and was used to analyze the obtained data. Some of the associated parameters obtained are given in Table 8. The goodness of the fits were in the order of 10^{-4} – 10^{-5} indicating good correlation with the $R_s(R_{ct}\emptyset_{CPE})$ equivalent circuit model used [50]. The surface roughness of the steel was compensated by introduction of a non-integer element dependent on frequency called constant phase element, CPE which can be estimated using Y_0 and n, related to impedance by:

$$Z_{CPE} = = (Y_0)^{-1}(jw)^{-n} \quad (11)$$

where Z_{CPE} is the impedance of the CPE, Y_0 is the CPE constant, w is the angular frequency, j is an imaginary complex number, $(j^2 = -1)\alpha$ is the phase angle of CPE and $n = 2\alpha/(\pi)$.

The value of n indicates deviation of the CPE and can be used to predict the degree of roughness or inhomogeneity of the steel surface. This value decreased on addition of 5-HTP suggesting that the surface roughness of the steel is increased by adsorption of inhibitor molecules on steel surface active sites [50]. It also shows that there is relative and/or integrated influence on the CPE: not just a single resistance, capacitance or inductive element. Decrease in *n* on addition inhibitors also signifies insulation of the metal/solution interface by formation of a surface film. Formation of this film results in increase in charge transfer resistance in the presence than absence of inhibitor. The charge transfer resistance increased with increase in inhibitor concentration showing that the 'blanketing' property of the film improved as inhibitor concentration increased. The inhibition efficiency obtained also increased with increase in inhibitor concentration, hence consistent with weight loss results.

Increase in peak heights of the Bode plots suggests more capacitive response of the interface due to the presence of adsorbed inhibitor layer [50]. This capacitive response can result from formation of an electrochemical double layer with a capacitance, and its magnitude (C_{dl}) was estimated using Eq. 6 earlier stated. The C_{dl} values decreased in the presence of inhibitors, similar to results obtained by Shaban and coworkers using vanillin cationic surfactants [51] and Anupama and coworkers using *Pimenta dioica* leaf extracts [50]. The

decrease in C_{dl} values can be attributed to decrease in the local dielectric or an increase in the thickness of the double layer or both, caused by the adsorbed protective film of the inhibitors as earlier inferred [33,50].

3.7 Potentiodynamic Polarization

Corrosion of iron in steel in HCl involves least one oxidation and one reduction process at each electrode, e.g.

$$\text{Anode: } Fe_{(s)} \longrightarrow Fe^{2+}_{(aq)} + 2e \quad (12)$$

$$\text{Cathode: } 2H^{+}_{(aq)} + 2e \longrightarrow H_{2(g)} \quad (13)$$

Partial anodic oxidation of the iron leads to its dissolution (corrosion) while hydrogen gas is liberated at cathode. The sum of both cathodic and anodic processes can be used to obtain the compromise or free corrosion potential (E_{corr}) and the corresponding current density (I_{corr}). Tafel cathodic and anodic constants (β_c and β_a) were obtained from the slope of Tafel polarization plots in Fig. 8. Some of the PDP parameters determined are shown in Table 9. The I_{corr} values decreased more with increase in inhibitor concentration due to formation of adsorbed protective film.

A displacement in E_{corr} to more positive values in the inhibited solutions compared to the free acid solution was observed in Fig. 8. In literature, when the corrosion potential is displaced in the negative direction, the inhibitor is regarded as cathodic whereas anodic inhibitors displace the potential in the positive direction [50]. Therefore, the shift to positive E_{corr} values suggests that the inhibitor have dominant influence on the partial anodic reaction. However, the highest shift from that of the free acid (δE_{corr}) was not up to -85mV, hence not sufficient to categorize the inhibitor is cathodic or anodic type. Similar shift in E_{corr} values (less than 85 mV) was reported [52] and the inhibitor was regarded as mixed type with anodic predominance. A mixed type inhibitor acts by blocking of some active anodic and cathodic sites of the metal without changing its dissolution or corrosion mechanism. In other words, 5-HTP inhibits both the iron dissolution and hydrogen evolution processes but more actively inhibiting iron oxidation which is anodic reaction.

The values of β_c and β_a obtained changes with concentration of inhibitor. Both values increase with increase in inhibitor concentration, with the highest value in the uninhibited solution. However, the highest difference between the values for the inhibited solutions from free acid solution was obtained with β_a. This also suggests that the inhibitor has anodic predominance [53]. The calculated inhibition efficiency also increased with increase in concentration of the inhibitor, similar to weight loss and EIS results. Also, the results obtained for EIS and PDP using 15% HCl (Table 10) are in good agreement.

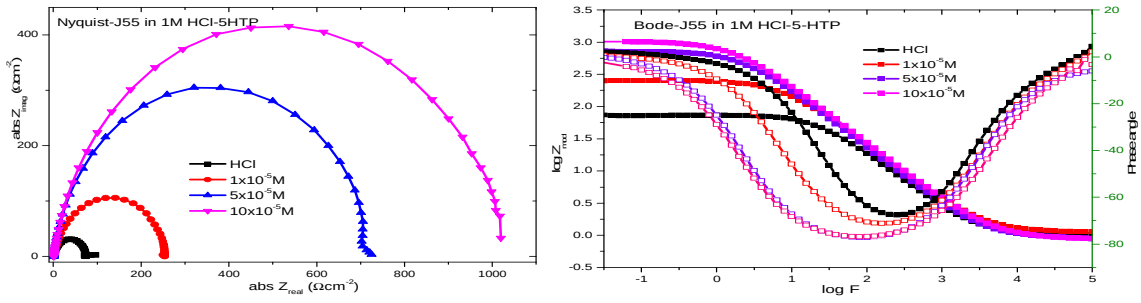

Fig. 6. Nyquist and Bode plots for inhibition of J55 steel corrosion in 1 M HCl using different concentrations of 5-HTP

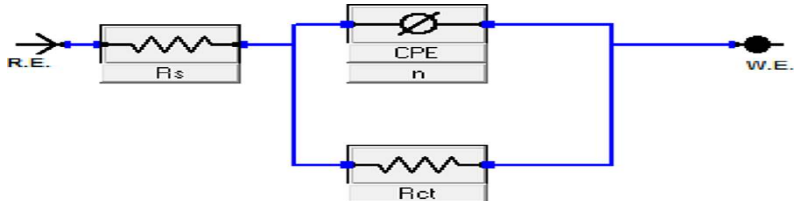

Fig. 7. Electrochemical equivalent circuit ($R_s\,(R_{ct}\emptyset_{CPE})$) model used for data fitting

Table 8. Some parameters obtained from EIS technique used to monitor the inhibition of J55 steel corrosion in 1 M HCl containing different concentrations of 5-HTP

EIS parameters	5-HTP concentration			
	0	1x10^{-5}	5x10^{-5}	10x10^{-5}
R_{ct} (Ωcm^2)	76.2	478.1	722.4	1021.0
R_s (Ωcm^2)	1.131	1.037	0.918	0.897
$Y_o x10^{-6}$ ($\Omega^{-1}s^n cm^{-1}$)	139.6	162.4	134.8	121.5
α ($x10^{-3}$)	872.2	892.7	905.2	983.1
Fit(x10^{-6})	131.1	10.5	19.8	11.7
N	0.555	0.551	0.548	0.517
$\mathbf{C_{dl}}$ x10^{-10} (Fcm^{-2})	3.51	1.24	0.11	0.03
$\boldsymbol{\varepsilon_{wl}}$ (%)	-	83.99	89.45	92.53

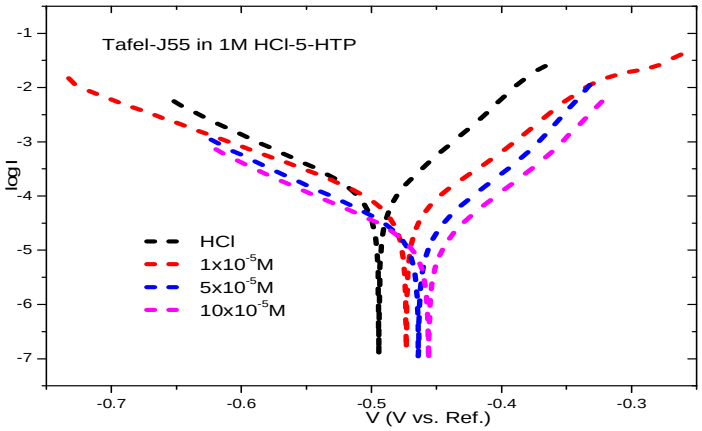

Fig. 8. Tafel plots for inhibition of J55 steel corrosion in 1 M HCl by 5-HTP at 30℃

Table 9. Some parameters obtained from PDP technique used to monitor the inhibition of J55 steel corrosion by 5-HTP at 30℃

PDP parameters	5-HTP concentration			
	0	1x10^{-5}	5x10^{-5}	10x10^{-5}
β_a (mV/decade)	71.3	52.1	55.0	55.2
β_c (mV/decade)	101.2	88.2	92.0	95.3
I_{corr} (μA)	619.4	88.0	49.1	12.7
E_{corr} (mV)	-473	-458	-464	-461
$\mathcal{E}_{PD}$ (%)	-	85.79	92.07	97.94

Table 10. Inhibition efficiency of 5-HTP obtained in 15% HCl solution by electrochemical measurements

Technique used	1x10^{-5} M	5x10^{-5} M	10x10^{-5} M	10x10^{-5} M + KI	10x10^{-5} M + PEG	10x10^{-5} M + NaG	10x10^{-5} M + GLU
EIS	61.2	65.4	71.1	86.8	88.2	75.4	89.8
PDP	65.1	69.9	80.0	88.4	90.6	76.1	91.2

3.8 Uv-visible Spectroscopy

Fig. 9 shows the spectral profile for IM HCl solution containing 1x10^{-5} M 5-HTP before and after immersion of J55 steel. The band obtained experienced a displacement in the presence of the inhibitor. This behavior has been ascribed to possible interaction between Fe^{2+} and inhibitor compounds in the inhibited solution [53]. Probable electronic transitions like $n \rightarrow \pi$ or $n \rightarrow \pi^*$ (involving non-bonding electrons of O and N) or $\pi \rightarrow \pi^*$ (involving multiple bonds and conjugated system) could have caused such displacement. In literature, when there is a shift

in position of the spectra of the solution after immersion of the metal, formation of a surface complex between the inhibitor and metal surface is inferred [54]. This complex acts as the adsorbed protective film that 'blankets' the steel surface from direct acid attack, hence corrosion inhibition.

3.9 FTIR Study

The spectrum of pure 5-HTP shows prominent peaks which provides insights on the functional groups in the compound. After immersion, some of the peaks are either lost or less prominent due to involvement of the corresponding functional group(s) in adsorption. Both spectra are plotted in Fig. 10 with the differences clearly observable. Those peaks around 3100-3300 cm^{-1}, 1600-1700 cm^{-1} and 1200-1300 cm^{-1} are worthy of note on the red line. The peak around 3100-3300 cm^{-1} can be assigned to either –OH or –NH vibrations: –OH vibrations could be broad in the presence of hydrogen bonding while $–NH_2$ is characterized by a single peak. These functional groups are available in the molecular structure of 5-HTP earlier shown in Fig. 1. The peak around 1600-1700 cm^{-1} is popularly assigned to C=O of an acid group which is available in the molecule. The peak around 1200-1300 cm^{-1} can be assigned to C-O group which is also present in the molecule. The disappearance of these peaks after immersion of the steel (see the blue line) demonstrates that these functional groups could have been actively involved in the adsorption process.

3.10 SEM/EDS Studies

To further establish the reliability of inferences drawn from FTIR results, EDS profiles of the surfaces of mild steel was obtained without and with formation of adsorbed film. The spectral profile of pure mild steel surface before immersion (Fig. 11, Left) shows presence of Fe, C, Si and O with no Cl. On immersion in 1M HCl, Fe slightly decreased, O slightly increased and Cl ions were detected (Fig. 11, Middle). The profile in the solution containing 5-HTP shows the highest O and N atoms (Fig. 11, Right) with reduced Cl. Thus, adsorption of the inhibitor on the surface involved mainly N and O atoms, and results in decreased iron exposure due to protective effect of the inhibitors. The decrease in Cl in the presence of 5-HTP indicates that some Cl ions are either displaced by the adsorbed inhibitor or forms a bridge-like structure between J55 surface and 5-HTP for adsorption of the inhibitor. This result is in agreement with observations made from FTIR studies.

Micrographs of an abraded steel coupon prior to immersion and that immersed in 1M HCl with and without 5-HTP for 24 hours were recorded by SEM. Result reveals that the surface of the abraded steel coupon (Fig. 12, Left) was considerably smooth with minimal attack or undulation. The surface of the coupon immersed in the free acid solution (Fig. 12, Middle) experienced severe damage due to corrosive attack leading to much pitting and undulation. However, the surfaces of the coupon immersed in the solution containing 5-HTP (Fig 12, Right) was relatively smoother compared to the free acid solution. This demonstrates that the addition of inhibitor reduces corrosive pitting which occurs in the free acid solution [55]. The extent of protection can be considered to be high since pitting decreases significantly. The protective layer formed by the inhibitor was not evenly distributed over the metal surface hence some portions of the surface were smoother than others. Thus, the active sites on the steel surface might not be equivalent or possess similar affinity for active molecules of the inhibitors. It could also be that adsorption of some molecules on the surface blankets the acid from attacking that portion by steric hindrance or micelles-like conformation of adsorbed molecules as described by [56]. Some cracks are visible in the protective layer (Fig 12 right) which may have been caused by surface cleaning before the specimen was scanned.

3.11 Adsorption Phenomenon of 5-HTP

Corrosion experts have presumed that CIs function by initial diffusion from bulk medium to the metal surface and subsequent adsorption on the metal surface. A schematic representation of this phenomenon is shown in Fig. 13.

Little effort has so far been made to explain the manner and speed of diffusion of these inhibitor molecules. However, the mechanism of adsorption is understood and has been a very active field of research. Four forms of adsorptive interactions that may take place at the metal-inhibitor interface are [57]:

- electrostatic interaction between charged metal surface and charged inhibitor molecules;
- interaction of uncharged electron pair (which may come from non-bonding

orbitals of hetero atoms) of the inhibitor molecules with the metal;
- interaction of pie-electrons with the metals; or
- a combination of two or more of the above.

The first case exemplifies physical adsorption mechanism; the next two are associated with chemical adsorption mechanism; and the last with mixed or physio-chemisorptions. Results from adsorption study above reveals that 5-HTP molecules were physically adsorbed on the steel surface. Physical adsorption (or physisorption) involves multilayer adsorption due to electrostatic forces of interaction between charged inhibitor species and charged surface. The associated heat of adsorption is low (not above 20 kJmol^{-1}) as obtained in this study. Desorption can take place at increased temperature as amount of adsorbed species decreases with increase in temperature. This may have resulted in decrease in K_{ads} values with increase in temperature as obtained in this study.

Both FTIR and EDS results have indicated that the adsorption process was facilitated by N and O functionalities. To further probe this, the structure of 5-HTP was optimized. The frontier molecular orbitals density and energy (namely LUMO and HOMO) of 5-HTP were obtained theoretically calculated using DFT at BL3YP basis set (Fig. 14). Materials studio 7.0 software was used for the computation. Results indicate that electron rich sites (HOMO) are concentrated around N and O atoms while the C=C sites

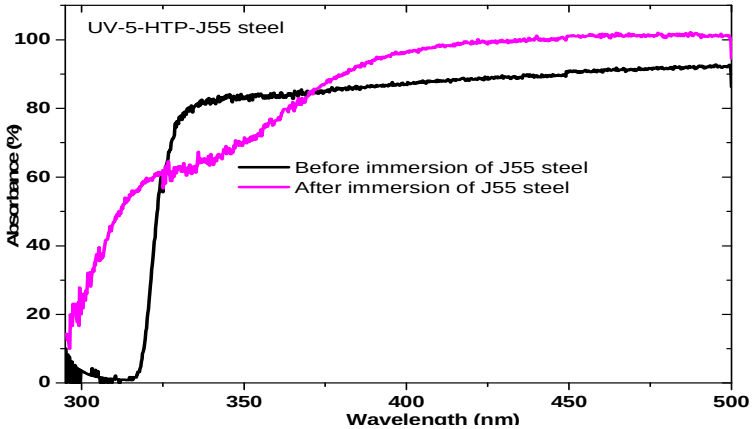

Fig. 9. UV-vis spectra of 1 M HCl containing 10x10^{-5} M HCl before and after immersion of J55 steel

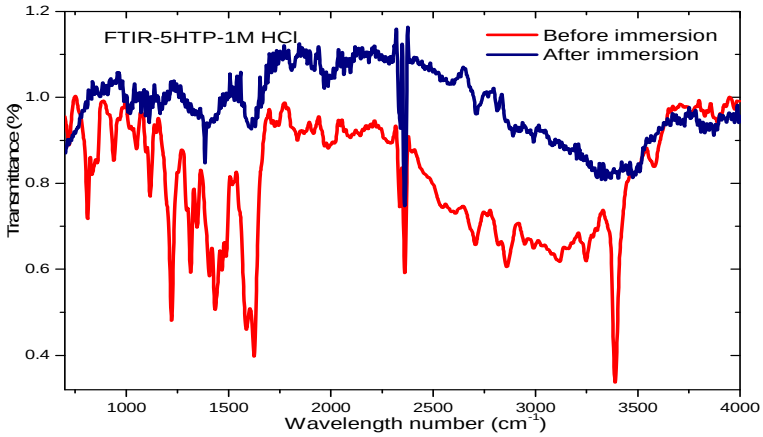

Fig. 10. FTIR spectra for 5-pure HTP and corrosion product after immersion of J55 steel

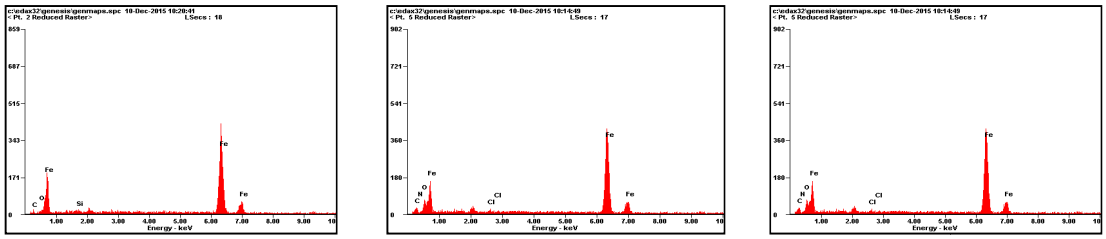

Element	Wt%	At%
CK	09.07	29.90
OK	02.80	06.93
SiK	00.99	01.40
FeK	87.13	61.77
Matrix	Correction	ZAF

Element	Wt%	At%
CK	09.41	30.82
NK	02.67	05.94
OK	08.75	17.06
ClK	03.61	04.54
FeK	75.56	41.64
Matrix	Correction	ZAF

Element	Wt%	At%
CK	08.41	28.83
NK	08.67	11.94
OK	11.75	19.06
ClK	00.61	00.54
FeK	70.56	39.63
Matrix	Correction	ZAF

Fig. 11. EDS spectra and spectral details of abraded J55 steel surface (Left), J55 immersed in 1 M HCl without (middle) and with 10x10^{-5} M 5-HTP

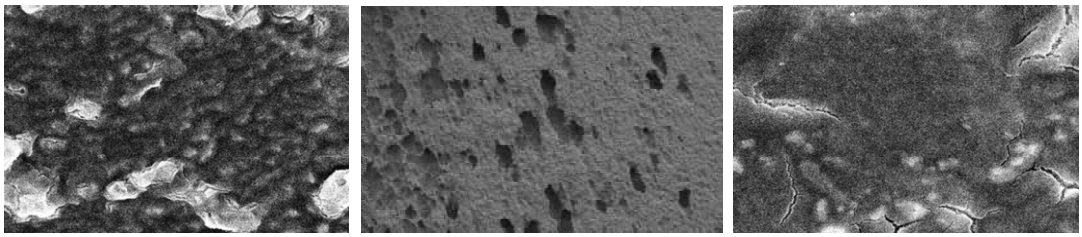

Fig. 12. Micrographs of abraded J55 steel (Left), J55 immersed in 1 M HCl only (Middle) and J55 steel immersed in 1 M HCl containing 10x10^{-5} M 5-HTP

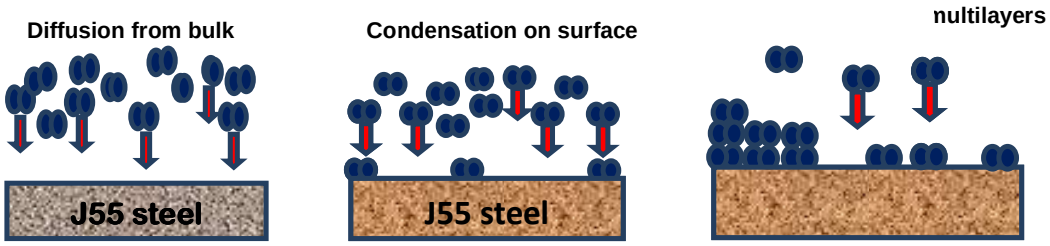

Fig. 13. Schematic representation of adsorption of molecules on solid surfaces from bulk phase

constitute the LUMO. The energies calculated were -1.497 eV and -3.211 eV for HOMO and LUMO respectively. A higher value of E_{HOMO} is likely to indicate a high tendency to donate electrons to appropriate acceptor molecule of low empty orbital energy and vice versa, therefore enhancing the inhibition efficiency [58]. Thus, electrostatic interactions between 5-HTP and the surface, which leads ability to inhibit the metal corrosion, occurs by means of O and N atoms. The band gap energy and dipole moment of 5-HTP obtained using Eq. 14 and 15 respectively are -1.724 eV and 7.919 Debye. Comparatively, these values are higher than some amino acid based CIs reported in literature [59,60] which could justify the high inhibition efficiency of 5-HTP.

$$\Delta E = E_{LUMO} - E_{HOMO} \quad (14)$$

$$\mu = q.r \quad (15)$$

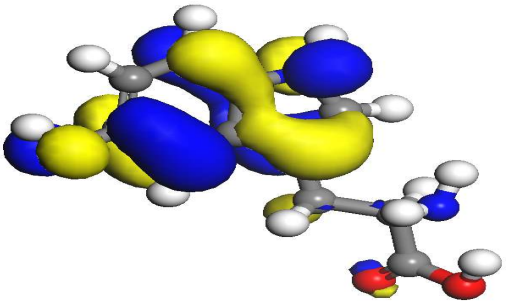

Fig. 14 (a). HOMO density of 5-HTP

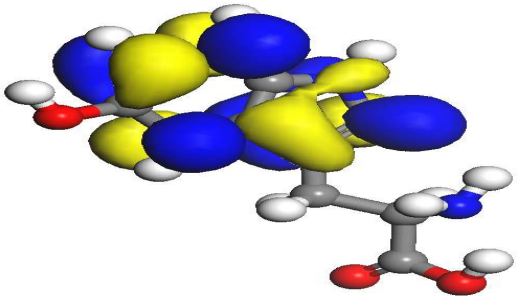

Fig. 14 (b). LUMO density of 5-HTP

4. CONCLUSION

5-HTP were investigated as anticorrosive oilfield chemical for J55 steel in acidic well treatment fluids. Inhibition efficiency of 5-HTP decreases from 91.4% and 73.9% in 1 M and 15% HCl respectively at 30℃ to 67.4% and 40.3% in the respective acid solutions at 90℃. Addition of potassium iodide and glutathione improves the efficiency to values above 87% and 72% in 1 M and 15% HCl respectively at 90℃. 5-HTP behaves as mixed type inhibitor with anodic predominance. Increase in 5-HTP concentrations decreases the double layer capacitance and increases the charge transfer resistance. 5-HTP inhibits mild steel corrosion by formation of protective film facilitated by O, N and C=C functionalities. 5-HTP is spontaneously physically adsorbed on J55 steel surface. Adsorption of 5-HTP is best approximated by Langmuir adsorption model. Adsorption of 5-HTP is also exothermic with resultant decrease in entropy of the bulk solution. Blends of 5-HTP with KI and GLU can be applied as alternative ecofriendly corrosion inhibitors for J55 steel materials in well treatment fluids containing HCl.

ACKNOWLEDGEMENTS

The authors acknowledge support from World Bank through the Robert S. McNamara Fellowship programme to conduct laboratory work abroad. We also appreciate Dr. Shuangqing Sun of Materials Physics and Chemistry Department, China University of Petroleum Qingdao for providing their facilities and softwares to carry out this research and African Centre of Excellence in Oilfield Chemicals Research for their support. EI is grateful to Prof. A. P. Udoh, Dr. B. S. Antia, Prof. Ogbona Joel, Prof. Hu, Dr. Li, Dr. Wang, Ubong Jerome, Chen, Chao, Xiang and Min in UPC for their assistance.

COMPETING INTERESTS

Authors have declared that no competing interests exist.

REFERENCES

1. Johannes KF. Petroleum engineer's guide to oil field chemicals and fluids. Gulf Professional Publishing; 2012.
2. Koch GH, Thompson NG, Virmani YP, Payer JH. Corrosion cost and preventive strategies in the United States; 2002.
3. Fink J. Petroleum engineer's guide to oil field chemicals and fluids. Chapter: Drilling Muds; 2011.
4. Obot IB. Recent advances in computational design of organic materials for corrosion protection of steel in aqueous media. Developments in Corrosion Protection, INTECH, Croatia. 2014;123-51.
5. Sangeetha M, Rajendran S, Muthumegala TS, Krishnaveni A. Green corrosion inhibitors–An overview. Zastis. Mater. 2011;52(1):3-11.
6. Uwah IE, Okafor PC, Ebiekpe VE. Inhibitive action of ethanol extracts from *Nauclea latifolia* on the corrosion of mild steel in H2SO4 solutions and their adsorption characteristics. Arab. J. Chem. 2013;6(3):285-293.
7. Finšgar M, Jackson J. Application of corrosion inhibitors for steels in acidic media for the oil and gas industry: A review. Corros. Sci. 2014;86:17-41.
8. El Azzouzi M, Aouniti A, Tighadouin S, Elmsellem H, Radi S, Hammouti B, El Assyry A, Bentiss F, Zarrouk A. Some hydrazine derivatives as corrosion inhibitors for mild steel in 1.0 M HCl: Weight loss, electrochemichal, SEM and theoretical studies. J. Mol. Liq. 2016;221: 633–641.

9. Gurudatt DM, Mohana KN, Tandon HC. Adsorption and corrosion inhibition characteristics of some organic molecules containing methoxy phenyl moiety on mild steel in hydrochloric acid solution. Mater. Disc.
DOI: 10.1016/j.md.2016.03.005
10. Xu C, Jin WL, Wang HL, Wu HT, Huang N, Li ZY, Mao JH. Organic corrosion inhibitor of triethylenetetramine into chloride contamination concrete by eletro-injection method. Const. Build. Mater. 2016;115: 602-617.
11. Verma C, Quraishi MA, Ebenso EE, Obot IB, El Assyry A. 3-Amino alkylated indoles as corrosion inhibitors for mild steel in 1 M HCl: Experimental and theoretical studies. J. Mol. Liq. 2016;219:647-660.
12. Yadava M, Kumar S, Sinha RR, Bahadurb I, Ebenso EE. New pyrimidine derivatives as efficient organic inhibitors on mild steel corrosion in acidic medium: Electrochemical, SEM, EDX, AFM and DFT studies. J. Mol. Liq. 2015;211:135-145.
13. Zakariaa K, Hamdya A, Abbas MA, Abo-Elenien OM. New organic compounds based on siloxane moiety as corrosion inhibitors for carbon steel in HCl solution: Weight loss, electrochemical and surface studies. J. Taiwan Inst. Chem. Eng. 2016; 65:530–543.
14. Odozi NW, Babalola JO, Ituen EB, Eseola AO. Imidazole derivative as novel effective inhibitor of mild steel corrosion in aqueous sulphuric acid. Amer. J. Phys. Chem. 2015;4(1):1-9.
15. Rani BE, Basu BBJ. Green inhibitors for corrosion protection of metals and alloys: An overview. Int. J. Corros; 2012.
16. Joel O. Tapping the untapped wealth in our backyard: Pathway to local content development. University of Port Harcourt Inaugural Lecture Series No. 104. 2013; 29-30.
17. Kavuric SR, Mukkamala SB. Estimation of 5-HTP in West African medicinal plant *Griffonia simplicifolia* Bail by ultra performance liquid chromatography. Int. J. Biol. Chem. Sci. 2010;4(2):520-523.
18. Kumar PS, Praven T, Jain N, Ndra BJ. A review of *Griffonia simplicifolia*-an ideal herbal antidepressant. Int. J. Pharm. Life Sci. 2010;1(3):174-181.
19. Adotey A, Nii J. Local production of 5-HTP from the seeds of *Griffonia simplicifolia.* Disserttion; 2009.
20. Larmie ET, Poston L. The *in vitro* effects of griffonin and ouabain on erythrocyte sodium content obtained from normal subjects and sickle cell patients. Plant Med. 1991;57(2):116-118.
21. Eckhardt AE, Malone BN, Goldstein IJ. Inhibition of ehrlich ascites tumor cell growth by *Griffonia simplicifolia* lectin *in vivo*. Cancer Res. 1982;42:2977-2979.
22. Frangatos G, Chubb FL. A new synthesis of 5-hydroxytryptophan. Canad. J. Chem. 1959;37(8):1374-1376.
23. Hara R, Kino K. Enhanced synthesis of 5-hydroxy-l-tryptophan through tetrahydropterin regeneration. AMB Expr. 2013;3(1):1-7.
24. Al-Baghdadi SB, Noori FTM, Ahmed WK, Al-Amiery AA. Thiadiazole as a potential corrosion inhibitor for mild steel in 1 M HCl. J. Adv. Electrochem. 2016;2(1):67-69.
25. Elyn Amira WAW, Rahim AA, Osman H, Awang K, Bothi Raja P. Corrosion inhibition of mild steel in 1 M HCl solution by *Xylopia ferruginea* leaves from different extract and partitions. Int. J. Electrochem. Sci. 2011;6:2998-3016.
26. Emregül KC, Atakol O. Corrosion inhibition of iron in 1 M HCl solution with schiff base compounds and derivatives. Mater. Chem. Phys. 2004;83(2):373-379.
27. Saha SK, Dutta A, Ghosh P, Sukul D, Banerjee P. Novel schiff base molecules as efficient corrosion inhibitors for mild steel surface in 1 M HCl medium: Experimental and theoretical approach. Phys. Chem. Chem. Phys. 2016;18: 17898-17911.
28. Kennedy JL. Oil and gas pipeline fundamentals. Pennwell Books; 1993
29. Masakatsu U, Takabe H, Nice PI. The development and implementation of a new alloyed steel for oil and gas production wells. Corros. 2000. NACE International; 2000.
30. El-Meligi A. Hydrogen production by aluminum corrosion in hydrochloric acid and using inhibitors to control hydrogen evolution. Int. J. Hydr. Ener. 2011;36(17): 10600-10607.
31. Finšgar M. 2-Mercaptobenzimidazole as a copper corrosion inhibitor: Part I. Long-term immersion, 3D-profilometry and electrochemistry. Corros. Sci. 2013;72;82-89.
32. Ahmad Z. Principles of corrosion engineering and corrosion control. Butterworth-Heinemann; 2006.

33. Rajeswari V, Kesavan D, Gopiraman M, Viswanathamurthi P, Poonkuzhali K, Palvannan T. Corrosion inhibition of *Eleusine aegyptiaca* and *Croton rottleri* leaf extracts on cast iron surface in 1 M HCl medium. Appl. Surf. Sci. 2014;314:537-545.
34. Singh P, Singh A, Quraishi M. Thiopyrimidine derivatives as new and effective corrosion inhibitors for mild steel in hydrochloric acid: Electrochemical and quantum chemical studies. J. Taiwan Inst. Chem. Eng. 2015;60:588-561.
35. Al-Otaibi MS, Al-Mayouf AM, Khan M, Mousa AA, Al-Mazroa SA, Alkhathlan HZ. Corrosion inhibitory action of some plant extracts on the corrosion of mild steel in acidic media. Arab. J. Chem. 2014; 7(3):340–346.
36. Abdel-Azim AA, Milad R, El-Ghazawy R, Kamal R. Corrosion inhibition efficiency of water soluble ethoxylated trimethylol propane by gravimetric analysis. Egypt. J. Petrol. 2014;23(1):15–20.
37. Akpabio I, Ejedawe J, Ebeniro J, Uko E. Geothermal gradients in the Niger Delta Basin from continuous temperature logs. Global J. Pure Appl. Sci. 2003;9(2):265-272.
38. Nwankwo CN, Ekine AS. Geothermal gradients in the Chad Basin, Nigeria, from bottom hole temperature logs. Int. J. Phys. Sci. 2009;4(12):777-783.
39. Adedapo J, Ikpokonte A, Schoeneich K, Kurowska E. An estimate of oil window in Nigeria Niger Delta Basin from recent studies. Gas. 2014;5(11):12-18.
40. Emujakporue G, Ekine A. Determination of geothermal gradient in the Eastern Niger Delta sedimentary basin from bottom hole temperatures. J. Earth Sci. Geotech. Eng. 2014;4(3):109-114.
41. Shukla SK, Ebenso EE. Corrosion inhibition, adsorption behavior and thermodynamic properties of streptomycin on mild steel in hydrochloric acid medium. Int. J. Electrochem. Sci. 2011;6:3277-329.
42. Umoren S, Solomon M. Effect of halide ions on the corrosion inhibition efficiency of different organic species–A review. Journal of Industrial and Engineering Chemistry. 2015;21:81-100.
43. Brezinski M. New environmental options for corrosion inhibitor intensifiers. Paper presented at the SPE/EPA Exploration and Production Environmental Conference; 1999.
44. Karthikaiselvi R, Subhashini S. Study of adsorption properties and inhibition of mild steel corrosion in hydrochloric acid media by water soluble composite poly (vinyl alcohol-o-methoxy aniline). J. Asso. Arab Uni. Basic Appl. Sci. 2014;16:74-82.
45. Mourya P, Banerjee S, Singh M. Corrosion inhibition of mild steel in acidic solution by *Tagetes erecta* (Marigold flower) extract as green inhibitor. Corros. Sci. 2014;85:352-363.
46. Alaneme KK, Olusegun SJ, Adelowo OT. Corrosion inhibition and adsorption mechanism studies of *Hunteria umbellata* seed husk extracts on mild steel immersed in acidic solutions. Alex. Eng. J. 2016; 55(1):673-681.
47. Khadom A, Yaro A, Al-Taie A, Kadum A. Electrochemical, activations and adsorption studies for the corrosion inhibition of low carbon steel in acidic media. Port. Electrochim. Acta. 2009;27(6): 699-712.
48. Hamdy A, El-Gendy NS. Thermodynamic, adsorption and electrochemical studies for corrosion inhibition of carbon steel by henna extract in acid medium. Egypt. J. Petrol. 2013;22(1):17-25.
49. Umoren SA, Obot IB, Ebenso EE, Okafor PC. Eco-friendly inhibitors from naturally occurring exudate gums for aluminium corrosion inhibition in acidic medium. Port. Electrochim. Acta. 2008;26(3):267-282.
50. Anupama KK, Ramya K, Shainy KM, Joseph A. Adsorption and electrochemical studies of *Pimenta dioica* leaf extracts as corrosion inhibitor for mild steel in hydrochloric acid. Mater. Chem. Phys. 2015;167:28-41.
51. Shaban SM, Aiad I, El-Sukkary MM, Soliman E, El-Awady MY. Inhibition of mild steel corrosion in acidic medium by vanillin cationic surfactants. J. Mol. Liq. 2015; 203:20-28.
52. Fouda AS, Shalabi SK, Elewady GY, Merayyed HF. Chalcone derivatives as corrosion inhibitors for carbon steel in 1 M HCl solutions. Int. J. Electrochem. Sci. 2014;9:7038–7058.
53. Olasunkanmi LO, Kabanda MM, Ebenso EE. Quinoxaline derivatives as corrosion inhibitors for mild steel in hydrochloric acid medium: Electrochemical and quantum chemical studies. Physica E. 2016;76:109-126.
54. Karim S, Mustafa CM, Asaduzzaman M, Islam M. Corrosion inhibition of mild steel

by calcium gluconate in simulated cooling water. Leon. Elec. J. Pract. Technol. 2010;9(16):167-176.

55. Gürten AA, Keleş H, Bayol E, Kandemirli F. The effect of temperature and concentration on the inhibition of acid corrosion of carbon steel by newly synthesized Schiff base. J. Indus. Eng. Chem. 2015;27:68-78.
56. Wang X, Liu L, Wang P, Li W, Zhang J, Yan Y. How the inhibition performance is affected by inhibitor concentration: A perspective from microscopic adsorption behavior. Ind. Eng. Chem. Res. 2014; 53(43):16785-16792.
57. Amar H, Benzakour J, Derja A, Villemin D, Moreau B, Braisaz T. Piperidin-1-yl-phosphonic acid and (4-phosphono-piperazin-1-yl) phosphonic acid: A new class of iron corrosion inhibitors in sodium chloride 3% media. Appl. Surf. Sci. 2006;252(18):6162–6172.
58. Khaled K, Amin MA. Computational and electrochemical investigation for corrosion inhibition of nickel in molar nitric acid by piperidines. J. Appl. Electrochem. 2008; 38(11):1609-1621.
59. Aouniti AK, Khaled KF, Hammouti B. Correlation between inhibition efficiency and chemical structure of some amino acids on the corrosion of armco iron in molar HCl. Int. J. Electrochem. Sci. 2013; 8:5925-5943.
60. Eddy NO, Momoh-Yahaya H, Oguzie EE. Theoretical and experimental studies on the corrosion inhibition potentials of some purines for aluminum in 0.1 M HCl. J. Adv. Res. 2015;6(2):203-217.

Peer-review history:
The peer review history for this paper can be accessed here:
http://sciencedomain.org/review-history/17573